Persistence of SARS-CoV-2 virus and viral RNA on hydrophobic and hydrophilic surfaces and investigating contamination concentration

Susan Paton[1], Antony Spencer[1], Isobel Garratt[1], Katy-Anne Thompson[1#], Ikshitaa Dinesh[1#], Paz Aranega-Bou[1], David Stevenson[1#], Simon Clark[1], Jake Dunning[2,3], Allan Bennett[1] and Thomas Pottage[1]*

[1]Public Health England, National Infection Service, Porton Down, Wiltshire, UK

[2]Emerging Infections and Zoonoses, National Infection Service, Public Health England

[3]NIHR Health Protection Research Unit in Emerging and Zoonotic Infections

*Correspondence: thomas.pottage@phe.gov.uk

#Author no longer work for PHE

Running title: Recovery of SARS-CoV-2 virus and RNA from surfaces

Abstract (229 of 250)

The transmission of SARS-CoV-2 is likely to occur through a number of routes, including contact with contaminated surfaces. Many studies have used RT-PCR analysis to detect SARS-CoV-2 RNA on surfaces but seldom has viable virus been detected. This paper investigates the viability over time of SARS-CoV-2 dried onto a range of materials and

22 compares viability of the virus to RNA copies recovered, and whether virus viability is
23 concentration dependant.

24 Viable virus persisted for the longest time on surgical mask material and stainless steel with
25 a 99.9% reduction in viability by 124 and 113 hours respectively. Viability of SARS-CoV-2
26 reduced the fastest on a polyester shirt, with a 99.9% reduction within 2.5 hours. Viability on
27 cotton was reduced second fastest, with 99.9% reduction in 72 hours. RNA on all the
28 surfaces exhibited a one log reduction in genome copy recovery over 21 days.

29 The findings show that SARS-CoV-2 is most stable on non-porous hydrophobic surfaces. RNA
30 is highly stable when dried on surfaces with only one log reduction in recovery over three
31 weeks. In comparison, SARS-CoV-2 viability reduced more rapidly, but this loss in viability
32 was found to be independent of starting concentration. Expected levels of SARS-CoV-2 viable
33 environmental surface contamination would lead to undetectable levels within two days.
34 Therefore, when RNA is detected on surfaces it does not directly indicate presence of viable
35 virus even at high CT values.

36

37 Importance (81 of 150)

38 This study shows the impact of material type on the viability of SARS-CoV-2 on surfaces. It
39 demonstrates that the decay rate of viable SARS-CoV-2 is independent of starting
40 concentration. However, RNA shows high stability on surfaces over extended periods. This
41 has implications for interpretation of surface sampling results using RT-PCR to determine the
42 possibility of viable virus from a surface. Unless sampled immediately after contamination it
43 is difficult to align RNA copy numbers to quantity of viable virus on a surface.

44

45

Keywords: SARS-CoV-2, Environmental persistence, COVID-19, Transmission, Surface sampling

Word count Abstract: 229

Word count manuscript: 3345

Introduction

Severe acute respiratory syndrome coronavirus 2 (SARS-CoV-2) causing coronavirus disease 2019 (COVID-19) has spread globally and many countries are experiencing ongoing local transmission despite varying levels of control efforts. SARS-CoV-2 is primarily transmitted via respiratory droplets from an infected host (1). Studies have confirmed aerosol viral transmission (2-4) with SARS-CoV-2 being shown to remain viable in aerosols for between 90 minutes and 3 hours in laboratory studies (5, 6). Infections from direct person to person transmission have been confirmed as well as indirect transmission through close contacts after tracing of case clusters (7, 8). It is suspected that contaminated surfaces or fomites may also have a role in transmission. Studies detailing SARS-CoV-2 viability on surfaces have contributed to this (6).

SARS-CoV-2 RNA has been detected on environmental surfaces, potentially indicating the presence of the viable virus (9, 10). Current environmental sampling of surfaces using swabs, primarily uses real-time PCR (RT-PCR) to detect viral genome in samples. Few studies have been able to isolate viable virus from environmental surface sampling, even where RT-PCR indicates a high level of SARS-CoV-2 RNA is present (11). Recent manuscripts have identified survivability ranges for SARS-CoV-2 on surfaces in the laboratory, with only one demonstrating the relationship between viable recovered virus and RNA on the surface (12, 13). As the risk of infection from of virus-contaminated surfaces is difficult to predict (14),

70 further investigation is required to enhance understanding on the survivability of SARS-CoV-
71 2 on surfaces.

72 The three aims of this study were; (i) measure the persistence of viable SARS-CoV-2 virus on
73 common personal protective equipment (PPE) materials (both hospital-grade and reusable
74 fabrics), high-touch surface materials and commonly worn fabrics; (ii) to investigate the
75 relationship between recoverable viable virus from these surfaces and the levels of SARS-
76 CoV-2 RNA in the same sample; (iii) determine the relationship between inactivation rate
77 and initial viral titre load on surfaces.

78

79 **Results**

80 SARS-CoV-2 viability decreased on all materials during the 2.5 hour drying period, on average
81 by 1.01 $\log_{10}$ (between -0.18 $\log_{10}$ for disposable gown to -3.66 $\log_{10}$ for polyester sports
82 shirt, standard deviation 1.06 $\log_{10}$) from a high starting inoculum of approximately 4 x 10^5
83 pfu per material. Viable virus could be recovered from the surgical mask and stainless steel
84 coupons for the longest periods of time ($\log_{10}$ reductions of 4.91 and 4.99, respectively, over
85 7 days). The recovery time for cotton t-shirt and polyester sports shirt materials was shorter
86 ($\log_{10}$ reductions of 5.15 over 5 days and 3.9 within 1 day). RNA copy number was recovered
87 at higher concentrations in all samples compared to the levels of viable virus, decreasing by
88 ~1.5 $\log_{10}$ (non-porous, hydrophobic) and ~1 $\log_{10}$ (porous, hydrophilic) over the initial 7
89 days, then stabilised at around $10^{7.5}$ copies per coupon from day 7. The ratio of viable virus
90 recovered ranged from 10^3 to 10^8 times less when compared to viral RNA assayed, from start
91 to finish of the study period (Fig 1).

92

93 Linear regression analysis was completed using the recoverable virus data to calculate time
94 for percentage reduction (Table 2). Regressions were calculated from t=2.5 hours

95 onwards. Calculated decay rate is fastest on cotton with a 99.9% reduction in recovery
96 within 72 hours. The longest survival of virus is observed on surgical mask material, where
97 124 hours is required for a reduction of 99.9%. For the polyester sports shirt a >3 $\log_{10}$
98 reduction was detected during the initial 2.5 hour timepoint (Table 2).
99
100 The results from the comparative study involving two viral titres revealed an initial rapid
101 decrease in the recovery of viable virus from the surface during the drying period, with the
102 inactivation rate decreasing after drying. Virus was recovered after four days for the low
103 inoculum and up to seven days for the high inoculum (Figure 2). Parallel survival rates of high
104 and low inocula demonstrate that the decay rate of SARS-CoV-2 is independent of
105 concentration when applied to a stainless steel surface ($P>0.05$).
106

107 **Discussion**

108 Contact with SARS-CoV-2 contaminated surfaces is thought to be a route of transmission in
109 the current pandemic (8, 15). Surfaces can be contaminated by virus-containing droplets
110 generated from an infected individual or contact with contaminated hands, with potential
111 onwards transmission via direct surface contact (16). With contamination events likely to
112 occur in a range of materials, this study investigated the survival of SARS-CoV-2 UK isolate
113 hCoV-19/England/2/2020 and associated viral RNA on a range of surfaces that are at risk
114 from droplet and touch contamination.

115 Existing studies examining time-based viability of SARS-CoV-2 on different surfaces have
116 focused on a single virus titre (6, 12, 13, 17). Our work investigated the persistence of high
117 titres of SARS-CoV-2 on various surfaces, and at two different titres on stainless steel
118 coupons with identical conditions.

119 When inoculated onto stainless steel, a five-log reduction in viability of the UK SARS-CoV-2
120 isolate England 02/2020 HCM/V/052 was observed over a 7 day period (Figure 1). Riddell *et*
121 *al* showed a similar $\log_{10}$ reduction at 28 days and Kasloff at 14 days, using the Australian
122 isolate Betacoronavirus/Australia/SA01/2020 and Canadian isolate hCoV-19/Canada/ON-
123 VIDO-01/2020 respectively (12, 17). In both studies, the viral propagate included additives
124 such as serum and mucin to mimic bodily secretions (12, 17). Where in this current study the
125 virus stock suspension was centrifuged to remove the majority of the cell debris, but
126 left salts and proteins from the growth media used to propagate the virus. The initial starting
127 inoculum concentration (between 10^5-10^6 pfu per surface) and environmental conditions of
128 temperature and RH are similar for the two previous studies and this study, demonstrating it
129 is likely that the differences observed in survival results could primarily arise from a
130 protective effect afforded by added serum/mucin and/or the different isolates used. Whilst
131 potentially artificially high, the starting inoculum in this current study provides the ability to
132 determine the inactivation characteristics of the virus on the different materials which a
133 lower starting inoculum may not.

134 Currently there are no published studies investigating inter-isolate differences in
135 environmental surface stability of SARS-CoV-2. A study investigating the stability of SARS-
136 CoV-1 (AY274119.3) and SARS-CoV-2 (nCoV-WA1-2020) by van Doremalen *et al* showed that
137 both were similar under their experimental test conditions (6). Chin *et al* have reported
138 similar findings to the work presented in our study using a comparable starting
139 inoculum, also without additional protein (13). Their results showed that infectious SARS-
140 CoV-2 was recovered from a banknote and stainless steel on days 4 and 7
141 respectively, compared to our results of recoverable virus on day 5 from the banknote and
142 recovery on day 7 from stainless steel. With little evidence of difference in environmental
143 stability between isolates of SARS-CoV-2 the addition of bovine serum albumin and mucin to

144 the inoculating suspensions indicates that additional protein provided a protective effect to
145 the virus during and after drying onto the surfaces (12, 13, 17).

146 Droplets on non-porous or hydrophobic surfaces dry in a beaded shape, giving a high
147 volume to surface area ratio. In such an environment, these droplets can produce a core-
148 shell structure (18), which can concentrate the virus particles, salts and organic material into
149 smaller clumps (19). Such clumping is seen often in nature due to association with cellular
150 matter or protein (20, 21). These closely associated virus particles are protected from
151 environmental pressures such as desiccation, UV and heat, which cause inactivation (20).
152 However, on porous or hydrophilic surfaces the droplets are absorbed into
153 the material across a larger surface area, which will lead to less clumping and to
154 the presentation of individual viral particles; this may confer less protection from the drying
155 effects of the environment, leading to a reduction in the viability of the virus.

156 Whilst other studies have designated materials as porous and non-porous, this may be an
157 oversimplification of the surfaces studied (12, 17). The surface of a surgical mask is porous
158 but is made up of overlapping hydrophobic fibres; similarly, Tyvek material is produced
159 with non-woven fibres of high density hydrophobic polyethylene, but presents microscopic
160 pores on the surface. In the context of our study, relatively low amounts of liquid are being
161 added to these surfaces. Thus, these small droplets of liquid cannot penetrate into the
162 materials, as their hydrophobicity ensures the droplets of liquids remain on the surface of
163 the material during the drying process; making the surfaces behave more like a non-
164 porous one. Our results show that the porous but hydrophobic surfaces of the surgical mask,
165 disposable gown and Tyvek coverall produce similar decay rates when compared to the non-
166 porous hydrophobic surfaces of stainless steel with a five $\log_{10}$ reduction in recovered
167 infectivity over 7 days. Viable SARS-CoV-2 was recovered from these surface materials over
168 longer periods of time compared to the truly porous and hydrophilic surfaces tested,

169 cotton and woven polyester. An exception was the hydrophobic polymer bank note, from
170 which viable virus was recovered at the limit of detection for days 5 and 7 of the study. This
171 is different to the study of Riddell *et al* where the recovery from the Australian bank note
172 was similar to the other non-porous surfaces tested (17). At present it is not clear why this
173 surface had decreased viability compared to the other non-porous hydrophilic surface used
174 in this study, although there may be antiviral properties from some of the dyes used in the
175 bank note.

176 Following a 4.73 $\log_{10}$ decrease, infectious virus was recovered from cotton material up to 3
177 days after inoculation; matching previous studies, reporting more rapid inactivation of virus
178 particles on cotton surfaces compared to others (12, 17). These results may be attributed to
179 two factors unrelated to any potential anti-viral activity of the material: retention of virus
180 within the cotton fibre matrix, or losses during the inoculum application due to wicking. Due
181 to the cotton's hydrophilic, woven nature, the liquid inoculum rapidly absorbs and
182 penetrates into the fibres which, when dried, might cause interactive forces, limiting the
183 release of virus particles, which is shown by a greater than 1 $\log_{10}$ reduction in recovery of
184 viable virus after the drying period. This decrease in detection of viable virus may therefore
185 be attributable to inefficient recovery from this specific type of material rather than
186 increased inactivation. This result indicates that viral particles may remain in cotton fibres
187 after contamination posing a forward transmission risk, but they will likely not be released
188 from the substrate to cause infection. To counteract the materials inherent absorbent
189 nature, during the inoculation and drying steps we suspended the cotton in strips across an
190 open box. Whilst this exposed the virus inoculated coupon to the environmental conditions
191 on both sides of the coupon it reduced any potential losses of the virus due to wicking on to
192 container surface from the coupon as seen in a previous study (12).

193 Though polyester, produced from polyethylene terephthalate, is hydrophobic, when spun
194 into fine fibres, aligned in the same orientation and woven into fabric, it behaved like the
195 other woven fabric tested, cotton. It is possible that the aligned polyester fibres which are
196 close together, but not fused, causes capillary action to draw the liquid into the interstitial
197 spaces between the fibres and trap the virus particles. Virus that was inoculated onto
198 polyester sports shirt was rapidly inactivated to unrecoverable levels in one day; there may
199 also be interaction between the chemicals used to process/colour the fabric and the virus
200 (22).

201 SARS-CoV-2 RNA has been detected on surfaces in different environments, but there have
202 been few reports of viable virus recovery from these surfaces. The use of RT-PCR to
203 determine the presence of SARS-CoV-2 on surfaces has advantages, increased sensitivity (RT-
204 PCR can detect small amounts of target RNA) and rapid high throughput of samples
205 compared to culture-based methods. The limitation of the use of RT-PCR in such studies is its
206 inability to distinguish between viable and non-viable virus.

207 The detection of SARS-CoV-2 RNA from surface samples is used to indicate that virus (viable
208 or non-viable) has been present on that surface at some point previously. Lower cycle
209 threshold (CT) values from the RT-PCR assay indicates that more copy numbers of target
210 RNA are present in that sample. Our study determined that a CT value of 18 equates to
211 approximately 5×10^8 copy numbers of the RNA target. The initial recovery of infectious
212 virus from the materials (Figure 1), excluding the polyester sports shirt, is approximately 3.1
213 $\log_{10}$ (SD 0.13 $\log_{10}$) lower than the copy number, showing that there is a large amount of
214 RNA exogenous to infection-competent viral particles in the inoculum. This
215 difference between infectious virus and RNA copy number was also reported by Kasloff *et al*
216 (12). The ratio between copy number and viable virus changes with time with recoverable
217 infectious virus rates reducing more rapidly than copy numbers recovered in the same

218 sample over time. The RNA is therefore more persistent in the environment compared with
219 infectious virus. It has been shown that SARS-CoV-2 RNA was detected on cruise ship
220 surfaces 17 days after cabins had been vacated (23).

221 Thus, it is not possible to draw conclusions on the viability of surface contamination from
222 genome copy number of RNA detected after the initial contaminating event. In addition,
223 the comparative persistence of RNA on the surfaces in comparison to infectivity makes it
224 difficult to relate copy number to the date when the contamination may have occurred.
225 Although our laboratory-based study used a concentration of infectious virus that may not
226 reflect the contamination load present in the environment, we demonstrated recovery of
227 viable virus at high and low concentrations.

228 Patient nasal and throat swab samples have produced CT values below 18 (24, 25), even to a
229 CT value of 10 (26), but reported surface samples have produced CT values above 28 (9, 27-
230 29). Using the results from our study to provide a calculation of the initial viable load on the
231 surface, a CT of 28 would provide an approximate infectious virus titre of 10^2 viral particles.
232 Using the recovery results from stainless steel as a representative surface in this study
233 (Figure 2), infectious virus from an initial recoverable inoculum of 10^2 viral particles would be
234 unrecoverable within 2 days. This is based on the vortex mixing recovery method used and
235 the detection would be thought to reduce further using direct surface sampling methods.
236 Future studies could address this limitation of knowledge where the copy number is
237 determined for much lower concentrations of SARS-CoV-2 on surfaces which will help to
238 further identify if the persistence of RNA is independent of concentration and addressing the
239 relationship to viable virus recovery.

240

241 Conclusions:

242 This study shows that the UK SARS-CoV-2 isolate, hCoV-19/England/2/2020, remains viable
243 on hydrophobic surfaces for up to 7 days, with recoverable viability on hydrophilic surfaces
244 reduced to 3 days at ambient temperature and relative humidity. Indicating that some
245 common surfaces could pose an infection risk if contaminated with high concentrations of
246 virus, although viable virus contamination levels of environmental surfaces are likely to be at
247 a low concentration. In contrast, recovery of RNA from the same samples shows little
248 reduction in copy numbers over the same period. The data presented also indicates that the
249 inactivation rate on environmental surfaces is independent of initial loading for SARS-CoV-2
250 and varies depending on surface type.

251

252 **Materials and methods**

253 *Viral isolate*

254 The SARS-CoV-2 isolate, England 02/2020 (EPI_ISL_407073) passage 3 (P3) used in this study
255 was propagated by the High Containment Microbiology Department at PHE, Porton Down.
256 The virus was isolated from a clinical sample taken during acute phase illness, using Vero E6
257 cells (ECACC, 85020206). A P2 master bank was produced using Vero E6 cells (BEI Resources,
258 NR-596) and a P3 working bank produced in Vero/hSLAM cells (ECACC 04091501). Cell lines
259 were infected at 95% confluence with an of MOI 0.0005 – 0.01 and maintained in 1x Minimal
260 Essential Medium GlutaMax, 4% heat-treated foetal bovine serum (Gibco), 1x non-essential
261 amino acids (Gibco), 25mM HEPES buffer (Gibco); additionally, Vero/hSLAM cells were also
262 maintained in the presence of 0.4mg/ml geneticin (ThermoFisher Scientific, Gibco). Virus
263 was harvested 3-6 days post-infection and supernatant clarified by centrifugation (3000 rpm,
264 10 min), virus was aliquoted and stored at -80oC. The titre of the P3 virus stock was
265 determined to be 2.0 x 107 pfu/ml by plaque assay. All work handling SARS-CoV-2 was
266 performed within a containment level 3 laboratory.

267

268 *Preparation of test surfaces*

269 The surfaces used in this study are representative of non-porous hand-touch sites (stainless
270 steel, 316 grade) and bank note (English polymer £10 note); PPE items used in the hospital
271 and wider environments (Multiple layered surgical mask, Tyvek coverall, disposable plastic
272 gown (37310 Breathable Impervious Gown)); and materials representing clothing items;
273 cotton t-shirt (Fruit of the Loom) and polyester sports shirt (85% polyester, 15% elastane,
274 Activewear SFP5-M02). 1cm x 1cm coupons of each material were prepared. Once prepared,
275 non-porous coupons (stainless steel and bank note) were cleaned with Neutracon (NEU5,
276 Scientific Laboratory Supplies, Nottingham, UK) detergent followed by rinsing with 70% IPA.
277 Additionally, stainless steel was sterilised by autoclaving. The surfaces not suitable for
278 cleaning (disposable plastic gown, cotton t-shirt, polyester sports shirt and Tyvek
279 coverall) were purchased new and handled aseptically. Materials were subdivided
280 depending on their surface properties, Table 1.

281

282 *Inoculation of test surfaces*

283 Viral aliquots were thawed to room temperature immediately prior to inoculation of the
284 materials. The stock suspension was diluted with cMEM to give a starting concentration of 4
285 x 10^7 and 4 x 10^5 pfu/ml for high and low loading, respectively. Coupons were inoculated by
286 the addition of 2 x 10µl droplets of virus culture within a negative pressure flexible film
287 isolator (FFI) and were left uncovered in plastic petri dishes in the FFI for the duration of the
288 study at a temperature of 21.5°C (±1°C) and an average relative humidity of 45%. Three
289 biological replicate coupons were prepared and inoculated for each time point (hours; 0, 2.5,
290 24, 48, 72, 96, 144, 168, 336 and 504) and each material. Triplicate coupons exposed but not
291 inoculated with the virus acted as negative controls.

292

293 *Recovery of SARS-CoV-2 from test surfaces*

294 Recovery of virus from the coupons at each specified timepoint was performed by
295 transferring a coupon into 1ml of cMEM in a 7ml bijou tube with 4 glass beads (3mm
296 diameter), followed by vortex mixing for 1 minute at maximum (Heidolph Multireax vortex).
297 The resulting suspension was transferred to a cryotube for storage at -80°C before analysis.
298 Storage of samples at -80°C was not found to affect viability of the virus or denature the RNA
299 (results not shown). Timepoint zero (t=0) coupons were recovered within 5 minutes of being
300 inoculated, before any drying occurred.

301

302 *Plaque Assay*

303 Coupon recovery liquid was assayed by thawing samples at room temperature, then serially
304 diluted (1 in 10) with MEM ((Gibco), 1% L-glutamine (Gibco), 1% Non-Essential Amino Acids
305 and 2.5% HEPES 1M). 100µl of each dilution was pipetted in duplicate (technical replicates),
306 up to four replicates for neat dilutions (400µ) onto confluent vero-E6 cells within a 24 well
307 plate (7.9 x 10^4 cells/cm^2). After one hour of incubation (±15 minutes) at 37°C with plate
308 rocking every 15 to 20 minutes, 0.5mL CMC overlay was added to each well; (1.5% CMC (3%
309 (w/v) carboxymethylcellulose solution in sterile distilled water (Sigma C4888)), 1% Antibiotic
310 Antimycotic Solution (100x) (Sigma Aldrich), 2x Overlay Media (20% 10x MEM (Gibco), 2% L-
311 glutamine (200mM) (Gibco), 2% Non-essential amino acids (Gibco), 6% Sodium bicarbonate
312 solution (Gibco), 8% Fetal bovine serum (Sigma Aldrich), 5% HEPES buffer (Gibco) and 57%
313 Distilled water (Versol). After 3 days incubation at 37°C, cells were fixed with formaldehyde
314 and stained by addition of approximately 250µl 0.2% crystal violet for 5 minutes, before
315 washing with water. The number of plaques in each well was determined and expressed as
316 plaque forming units (pfu).

317

318 *RNA extraction and RT-PCR Analysis*

319 RNA was extracted from aliquots (140 µL) of the coupon recovery liquid using the QIAamp
320 Viral RNA Mini Kit (Qiagen Ltd, Manchester, UK). RT-PCR was performed using the VIASURE
321 SARS-CoV-2 Real Time PCR Detection Kit (Viasure; CerTest Biotec, Zaragoza, Spain), following
322 the methods provided. Quantification was undertaken using the N target with a standard
323 curve generated by serial dilution of an *in vitro* transcript (10).
324
325
326 *Data Analysis*
327 Each time point for each material coupon had 3 biological replicates (individual coupons)
328 and 2 technical replicates (plaque assay performed in duplicate). Calculations for the mean
329 and standard deviations of the assay counts were determined from these 6 replicates using
330 Microsoft Excel (Office 365). Time to percent reduction values were calculated using linear
331 regression of pfu/coupon averages, in Minitab 18. High and low loading line slopes were
332 analysed using linear regression analysis with GraphPad Prism software version 7.
333

334 Funding

335 MRC award COV220-143 COVID-19: Understanding environmental and airborne routes of
336 transmission"

337

338 Conflict of interest

339 The authors do not have any conflict of interests.

340

341 Acknowledgements:

342 Professor K Richards in High Containment Microbiology, PHE, Porton Down, for producing
343 the viral stocks for this study.

344 The views expressed in this article are those of the authors and are not necessarily those of
345 PHE or the Department of Health and Social Care. This manuscript is Crown copyright and is
346 reproduced with the permission of Public Health England and the Controller of HMSO.

347

348 **References:**

349 1. Han Q, Lin Q, Ni Z, You L. 2020. Uncertainties about the transmission routes of 2019
350 novel coronavirus. Influenza Other Respir Viruses 14:470-471.
351 2. Stadnytskyi V, Bax CE, Bax A, Anfinrud P. 2020. The airborne lifetime of small speech
352 droplets and their potential importance in SARS-CoV-2 transmission. Proc Natl Acad
353 Sci U S A 117:11875-11877.
354 3. Ma J, Qi X, Chen H, Li X, Zhang Z, Wang H, Sun L, Zhang L, Guo J, Morawska L,
355 Grinshpun SA, Biswas P, Flagan RC, Yao M. 2020. COVID-19 patients in earlier stages
356 exhaled millions of SARS-CoV-2 per hour. Clin Infect Dis doi:10.1093/cid/ciaa1283.
357 4. Zhang R, Li Y, Zhang AL, Wang Y, Molina MJ. 2020. Identifying airborne transmission
358 as the dominant route for the spread of COVID-19. Proc Natl Acad Sci U S A
359 117:14857-14863.
360 5. Smither SJ, Eastaugh LS, Findlay JS, Lever MS. 2020. Experimental aerosol survival of
361 SARS-CoV-2 in artificial saliva and tissue culture media at medium and high humidity.
362 Emerg Microbes Infect 9:1415-1417.
363 6. van Doremalen N, Bushmaker T, Morris DH, Holbrook MG, Gamble A, Williamson
364 BN, Tamin A, Harcourt JL, Thornburg NJ, Gerber SI, Lloyd-Smith JO, de Wit E,
365 Munster VJ. 2020. Aerosol and Surface Stability of SARS-CoV-2 as Compared with
366 SARS-CoV-1. N Engl J Med 382:1564-1567.

367 7. Chan JF, Yuan S, Kok KH, To KK, Chu H, Yang J, Xing F, Liu J, Yip CC, Poon RW, Tsoi
368 HW, Lo SK, Chan KH, Poon VK, Chan WM, Ip JD, Cai JP, Cheng VC, Chen H, Hui CK,
369 Yuen KY. 2020. A familial cluster of pneumonia associated with the 2019 novel
370 coronavirus indicating person-to-person transmission: a study of a family cluster.
371 Lancet 395:514-523.
372 8. Cai J, Sun W, Huang J, Gamber M, Wu J, He G. 2020. Indirect Virus Transmission in
373 Cluster of COVID-19 Cases, Wenzhou, China, 2020. Emerg Infect Dis 26:1343-1345.
374 9. Zhou J, Otter JA, Price JR, Cimpeanu C, Garcia DM, Kinross J, Boshier PR, Mason S,
375 Bolt F, Holmes AH, Barclay WS. 2020. Investigating SARS-CoV-2 surface and air
376 contamination in an acute healthcare setting during the peak of the COVID-19
377 pandemic in London. Clin Infect Dis doi:10.1093/cid/ciaa905.
378 10. Moore G, Rickard H, Stevenson D, Bou PA, Pitman J, Crook A, Davies K, Spencer A,
379 Burton C, Easterbrook L, Love HE, Summers S, Welch SR, Wand N, Thompson KA,
380 Pottage T, Richards KS, Dunning J, Bennett A. 2020. Detection of SARS-CoV-2 within
381 the healthcare environment: a multicentre study conducted during the first wave of
382 the COVID-19 outbreak in England. J Hosp Infect doi:10.1016/j.jhin.2020.11.024.
383 11. Ahn JY, An S, Sohn Y, Cho Y, Hyun JH, Baek YJ, Kim MH, Jeong SJ, Kim JH, Ku NS,
384 Yeom JS, Smith DM, Lee H, Yong D, Lee YJ, Kim JW, Kim HR, Hwang J, Choi JY. 2020.
385 Environmental contamination in the isolation rooms of COVID-19 patients with
386 severe pneumonia requiring mechanical ventilation or high-flow oxygen therapy. J
387 Hosp Infect 106:570-576.
388 12. Kasloff SB, Leung A, Strong JE, Funk D, Cutts T. 2021. Stability of SARS-CoV-2 on
389 critical personal protective equipment. Sci Rep 11:984.
390 13. Chin AWH, Chu JTS, Perera MRA, Hui KPY, Yen HL, Chan MCW, Peiris M, Poon LLM.
391 2020. Stability of SARS-CoV-2 in different environmental conditions. Lancet Microbe
392 1:e10.

393 14. Casanova LM, Jeon S, Rutala WA, Weber DJ, Sobsey MD. 2010. Effects of air
394 temperature and relative humidity on coronavirus survival on surfaces. Appl Environ
395 Microbiol 76:2712-7.
396 15. Kanamori H, Weber DJ, Rutala WA. 2020. The role of the healthcare surface
397 environment in SARS-CoV-2 transmission and potential control measures. Clin Infect
398 Dis doi:10.1093/cid/ciaa1467.
399 16. Rheinbaben F, Schunemann S, Gross T, Wolff MH. 2000. Transmission of viruses via
400 contact in ahousehold setting: experiments using bacteriophage straight phiX174 as
401 a model virus. J Hosp Infect 46:61-6.
402 17. Riddell S, Goldie S, Hill A, Eagles D, Drew TW. 2020. The effect of temperature on
403 persistence of SARS-CoV-2 on common surfaces. Virol J 17:145.
404 18. You Y, Renbaum-Wolff L, Carreras-Sospedra M, Hanna SJ, Hiranuma N, Kamal S,
405 Smith ML, Zhang X, Weber RJ, Shilling JE, Dabdub D, Martin ST, Bertram AK. 2012.
406 Images reveal that atmospheric particles can undergo liquid-liquid phase
407 separations. Proc Natl Acad Sci U S A 109:13188-93.
408 19. Vejerano EP, Marr LC. 2018. Physico-chemical characteristics of evaporating
409 respiratory fluid droplets. J R Soc Interface 15.
410 20. Block SS. 2020. Disinfection, Sterilization and Preservation, 6th ed. Lippincott,
411 Williams and Wilkins.
412 21. Gerba CP, Betancourt WQ. 2017. Viral Aggregation: Impact on Virus Behavior in the
413 Environment. Environ Sci Technol 51:7318-7325.
414 22. Abedi. D, Mortazavi. SM, Mehrizi. MK, M F. 2008. Antimicrobial Properties of Acrylic
415 Fabrics Dyed with Direct Dye and a Copper Salt. Textile Research Journal 78:311-319.
416 23. Yamagishi T, Ohnishi M, Matsunaga N, Kakimoto K, Kamiya H, Okamoto K, Suzuki M,
417 Gu Y, Sakaguchi M, Tajima T, Takaya S, Ohmagari N, Takeda M, Matsuyama S,
418 Shirato K, Nao N, Hasegawa H, Kageyama T, Takayama I, Saito S, Wada K, Fujita R,

419 Saito H, Okinaka K, Griffith M, Parry AE, Barnetson B, Leonard J, Wakita T. 2020.
420 Environmental Sampling for Severe Acute Respiratory Syndrome Coronavirus 2
421 During a COVID-19 Outbreak on the Diamond Princess Cruise Ship. J Infect Dis
422 222:1098-1102.
423 24. Zou L, Ruan F, Huang M, Liang L, Huang H, Hong Z, Yu J, Kang M, Song Y, Xia J, Guo Q,
424 Song T, He J, Yen HL, Peiris M, Wu J. 2020. SARS-CoV-2 Viral Load in Upper
425 Respiratory Specimens of Infected Patients. N Engl J Med 382:1177-1179.
426 25. Arons MM, Hatfield KM, Reddy SC, Kimball A, James A, Jacobs JR, Taylor J, Spicer K,
427 Bardossy AC, Oakley LP, Tanwar S, Dyal JW, Harney J, Chisty Z, Bell JM, Methner M,
428 Paul P, Carlson CM, McLaughlin HP, Thornburg N, Tong S, Tamin A, Tao Y, Uehara A,
429 Harcourt J, Clark S, Brostrom-Smith C, Page LC, Kay M, Lewis J, Montgomery P, Stone
430 ND, Clark TA, Honein MA, Duchin JS, Jernigan JA, Public H-S, King C, Team CC-I. 2020.
431 Presymptomatic SARS-CoV-2 Infections and Transmission in a Skilled Nursing Facility.
432 N Engl J Med 382:2081-2090.
433 26. Lee L, Rozmanowski S, Pang M, Charlett A, Anderson C, Hughes G, Barnard M, Peto L,
434 Vipond R, Sienkiewicz A, Hopkins S, Bell J, Crook D, Gent N, Walker A, Eyre D, Peto T.
435 2021. An observational study of SARS-CoV-2 infectivity by viral load and
436 demographic factors and the utility lateral flow devices to prevent transmission.
437 Preprint.
438 27. Ong SWX, Tan YK, Chia PY, Lee TH, Ng OT, Wong MSY, Marimuthu K. 2020. Air,
439 Surface Environmental, and Personal Protective Equipment Contamination by Severe
440 Acute Respiratory Syndrome Coronavirus 2 (SARS-CoV-2) From a Symptomatic
441 Patient. JAMA 323:1610-1612.
442 28. Orenes-Pinero E, Bano F, Navas-Carrillo D, Moreno-Docon A, Marin JM, Misiego R,
443 Ramirez P. 2021. Evidences of SARS-CoV-2 virus air transmission indoors using
444 several untouched surfaces: A pilot study. Sci Total Environ 751:142317.

445 29. Ding Z, Qian H, Xu B, Huang Y, Miao T, Yen HL, Xiao S, Cui L, Wu X, Shao W, Song Y,
446 Sha L, Zhou L, Xu Y, Zhu B, Li Y. 2021. Toilets dominate environmental detection of
447 severe acute respiratory syndrome coronavirus 2 in a hospital. Sci Total Environ
448 753:141710.

449

450 *Table 1. Materials used in this study.*

451

452 *Fig 1. Mean quantities of viable virus recovered (pfu/coupon, orange) and viral RNA detected*
453 *(genome copy number/coupon, blue), for 7 materials assessed. Error bars represent the*
454 *standard deviation from three replicates. Grey dashed line represents the limit of detection of*
455 *the plaque assay for the combined assays from the triplicate coupons (0.8 pfu/ml). For Tyvek*
456 *coverall and disposable gown, 21 day coupons were not processed.*

457

458 *Table 2. Time for percentage reduction values for the multi-surface study. Data is sorted in*
459 *descending order by time to 99.9% survival rates. N/A = not applicable.*

460

461 *Fig 2. Virus viability results from loading of high (4 x 10^5 pfu added, blue) and low (4 x 10^3 pfu*
462 *added, red) SARS-CoV-2 inoculum onto stainless steel coupons (n = 3). Dashed lines show*
463 *linear regression based on recovery over time.*

464

465

466

467

468

469

Material	Properties
Stainless steel, Tyvek, disposable gown, bank note	Hydrophobic, non-porous
Surgical mask	Hydrophobic, porous
Cotton T-shirt, polyester sports shirt	Hydrophilic, porous

Table 1. Materials used in this study.

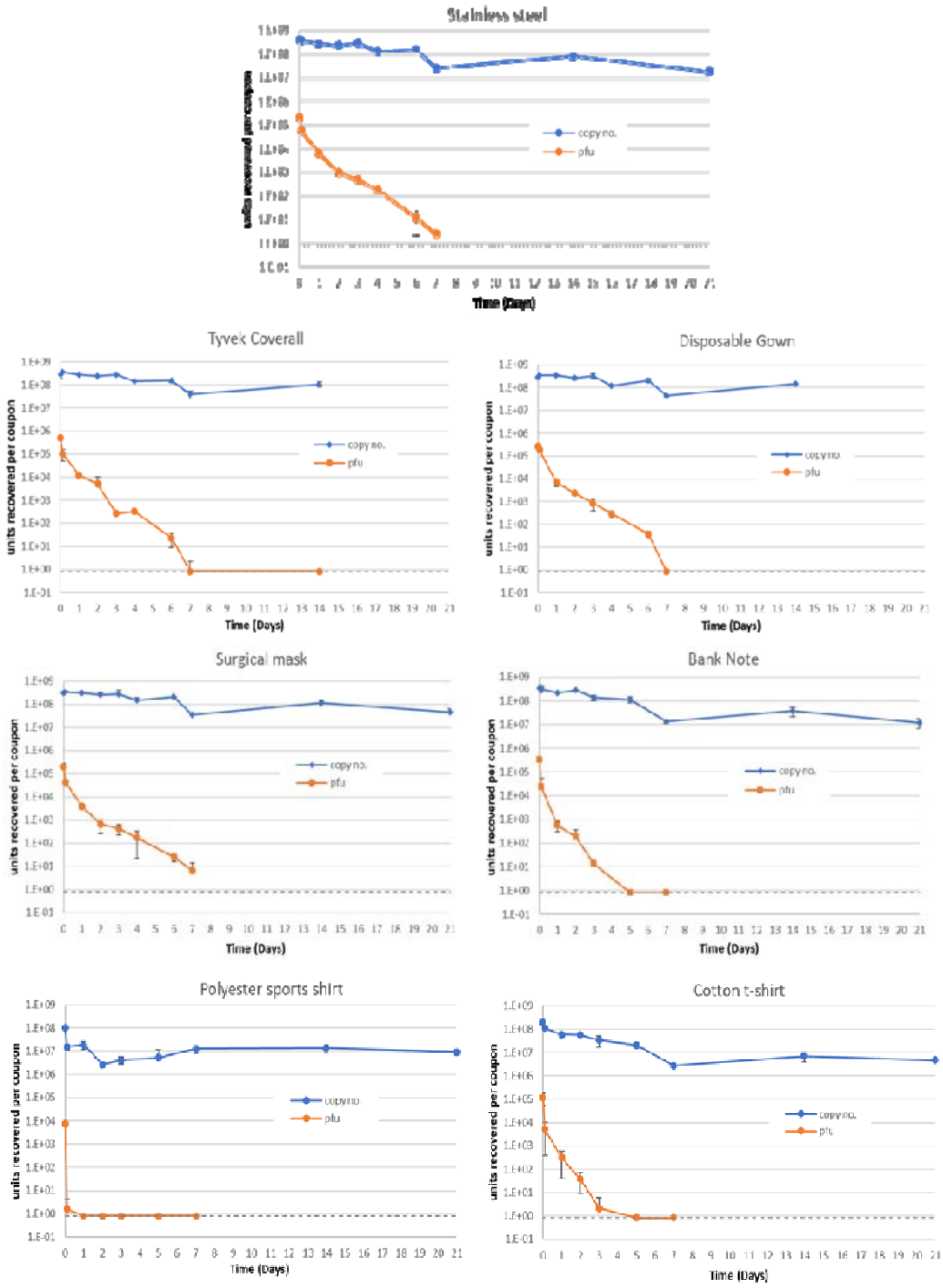

Fig 1. Mean quantities of viable virus recovered (pfu/coupon, orange) and viral RNA detected (genome copy number/coupon, blue), for 7 materials assessed. Error bars represent the standard deviation from three replicates. Grey dashed line represents the limit of detection of the plaque assay for the combined assays from the triplicate coupons (0.8 pfu/ml). For Tyvek coverall and disposable gown, 21 day coupons were not processed.

Material	Log change after 2.5 hour drying	Time for percentage reduction (hours)			
		R^2 value	90%	99%	99.9%
Surgical mask	-0.64	0.954	27.9	76.2	124.4
Stainless steel	-0.56	0.982	30.7	71.6	112.6
Tyvek Coverall	-0.70	0.962	33.3	69.3	105.2
Disposable Gown	-0.18	0.946	23.0	59.7	96.5
Bank note	-1.13	0.956	17.5	45.1	72.7
Cotton t-shirt	-1.34	0.904	17.2	44.6	72.0
Polyester sports shirt	-3.66	N/A		<2.5	

Table 2. Time for percentage reduction values for the multi-surface study. Data is sorted in descending order by time to 99.9% survival rates. N/A = not applicable.

483

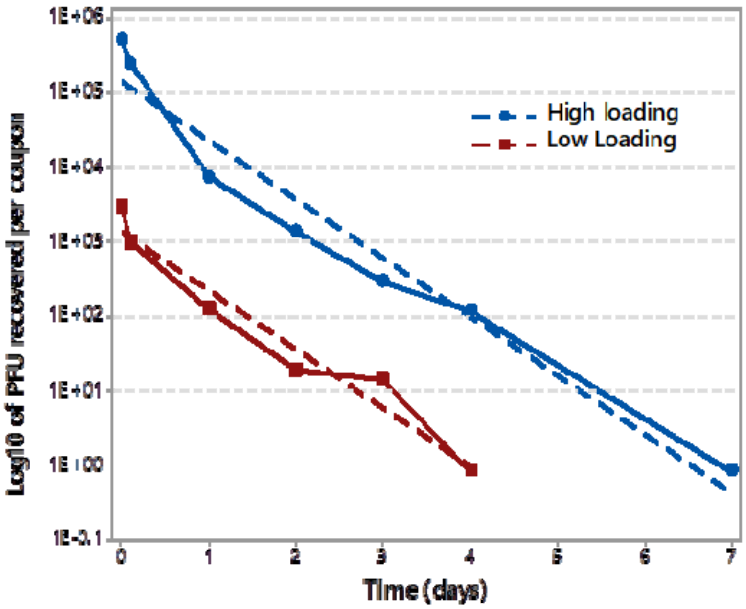

484

485 Fig 2. Virus viability results from loading of high (4 x 10^5 pfu added, blue) and low (4 x 10^3 pfu

486 added, red) SARS-CoV-2 inoculum onto stainless steel coupons (n = 3). Dashed lines show

487 linear regression based on recovery over time.

488

489